On the horizontal movement of thermal updrafts and their drag coefficient in windy weather

Oliver Predelli
oliver@gliderpilot.eu
Braunschweig, Germany

Abstract

In meteorology and in numerous publications on gliding, thermals are described as a phenomenon where air near the ground heats up, and this warm air drifts horizontally over the ground before ascending at a lifting edge. The evolving updraft column then is tilted by the wind. However, the analysis of GPS data from gliders and data from boundary layer measurement masts shows a completely different scenario. Thermal updrafts within the convective layer are vertically oriented even in the presence of wind. They move horizontally forward at the speed at which they detach from the ground. Updraft columns must be regarded as predominantly frictionless and have a drag coefficient of zero or nearly zero.

Nomenclature

A	cross-sectional area of an air parcel in m²
c_D	drag coefficient
D	drag force in N
F_I	inertia force in N
F_W	wind force in N
h	height in m
m	mass of the air parcel in kg
p	air pressure in Pa
p_0	standard air pressure, here p_0 = 1000 hPa
r	radius of the thermal updraft in m
R_d	specific gas constant of dry air (287.058 J/kgK)
T_P	temperature of the ascending air parcel in K
T_{pot}	potential temperature in K
T_v	virtual temperature in K
T_0	zero degree Celsius (T_0 = 273.15 K)
v_B	horizontal velocity of an air parcel in the thermal updraft in m/s
$v_{B,0}$	horizontal velocity of an air parcel when lifting off the ground in m/s
v_W	wind speed in m/s
V	volume of the air parcel in m³
w_G	climb rate of the glider in m/s
w_P	updraft velocity of the thermal in m/s
x	horizontal distance in m
δ_{entr}	parameter for dynamic entrainment in 1/s
ϑ_A	temperature of environmental air in °C
θ	potential temperature in °C
θ_V	virtual potential temperature in °C
λ_{entr}	parameter for lateral entrainment in 1/s
μ	mixing ratio in g/kg
ρ_A	density of environmental air kg/m³
ρ_P	density of the ascending air parcel in kg/m³
ρ_{pot}	potential density of an air parcel in kg/m³
τ_A	dew point temperature of the ambient air in °C
τ_P	dew point temperature of the thermal in °C

This article was peer reviewed by two independent, anonymous reviewers.

Introduction

Figure 1 illustrates the typical representation of an updraft, commonly found in both meteorological publications and gliding literature. It is assumed that air near the ground warms up and is pushed horizontally by the wind. The predominant warming takes place over dry fields or other easily heatable surfaces, such as urban areas. At an edge, such as the edge of a forest, this warmed air is lifted upward. It detaches from the ground and rises. Even in windy conditions, the updraft is fed from this detachment point. As gliders move with the wind while circling in thermals, it is also assumed that the thermal tilts sideways, under the influence of the wind. Graphics showing the inclined thermal can be found in the "Glider Flying Handbook" [1]. On windy days pilots are advised here to "...if heading toward a circling glider but at a thousand feet lower, estimate how much the thermal is tilted in the wind and head for the most likely spot upwind of the circling glider" [1].

In addition to updrafts detaching from a fixed point, gliding literature also describes the phenomenon of drifting thermals. Reichmann discusses this, stating, "If the wind is strong and the terrain is uniform, the lower turbulent layer itself induces thermal activity without being bound to any specific fixed ground points. Such thermals then stand relatively vertically and migrate with the wind across the land until the unstable air mass from the turbulent layer is depleted." But he generally assumes inclined updrafts in other cases, stating, "If a fixed point on the

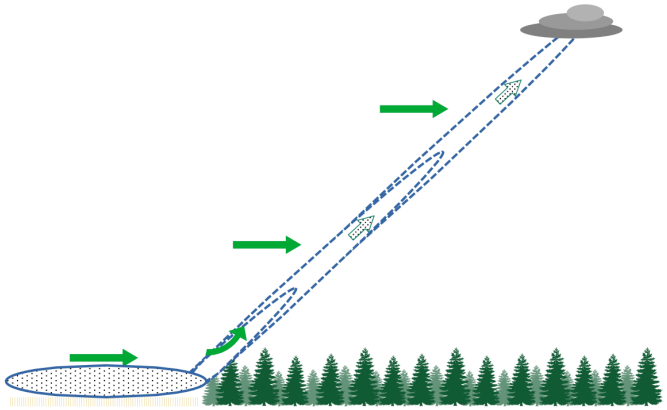

Fig. 1: The classical depiction of an updraft tilted by the wind in gliding literature.

ground triggers a larger thermal reservoir, the ascending warm air is carried away with the wind. Therefore, we must assume that in windy conditions, thermals originating from fixed ground sources ascend at an angle" [2]. According to Kottmeier, "In the case of thermals migrating with the flow, the updrafts, especially in the upper part of the thermally mixed height range, have an almost vertical trajectory" [3]. However, even in this context, an inclined thermal column is postulated: "The updraft area is inclined with the wind, causing the glider, which rises slightly slower than the air (due to its own sinking rate), to easily fall out of the updraft."

Childress measured thermal updrafts with a glider and, based on his data analysis, concludes, "the downwind side of convection cells in general had stronger and bigger updraft portions, lending credence to the theory that horizontal winds do not weaken the vertical updrafts, but tilt them with the wind" [4].

In contrast, Eckey is convinced that thermals ascend vertically. "It seems to be undisputed by now that most thermals stand approximately vertical, although a significant portion of older gliding literature assumes inclined thermal columns." In another passage, he states, "In any case, it is to be noted that thermal updrafts drift as nearly vertical columns with the wind" [5].

Bencatel et al. compare various models of atmospheric flow field phenomena and conclude that wind influence "may lean the thermal, move it, or both." In uneven terrain, there is a tendency for an updraft to be anchored as a "hot spot" on the ground or to migrate more slowly than the wind speed, with a tendency to lean leeward. Furthermore, they state, "During a thermal soaring flight, thermal leaning is sometimes wrongly perceived as a drift by the whole thermal" [6]. However, the leaning of the updraft is described only phenomenologically with trigonometric equations, lacking a physical justification.

If an updraft tilts under the influence of wind aloft, the wind must be capable of exerting a horizontal force on the thermal column. According to the laws of aerodynamics, this force implies the existence of a non-zero drag coefficient c_D. The thermal column then would act as an aerodynamic resistance on the horizontal wind flowing around it. In this consideration, we disregard any potential downwash caused by ground-level turbulence or lee effects from buildings, as described by Briggs [7], since thermals ascend many thousands of meters, and those phenomena have no influence at higher altitudes.

During the vertical ascent of thermals, when the updraft rises into the upper layers of the atmosphere, there are various, sometimes conflicting statements in the literature regarding the magnitude of the drag coefficient c_D. Several publications have analyzed the extent to which the rise of a thermal plume (or thermal column) is influenced by a drag coefficient at its head. Hernandez-Deckers and Sherwood, for example, are of the opinion that "The main force opposing buoyancy is a non-hydrostatic pressure drag, not mixing of momentum. This drag can be expressed in terms of a drag coefficient c_D that decreases as convection intensifies: deep convective thermals are less damped, with $c_D \sim 0.2$, while shallow convective thermals are more damped, with $c_D \sim 0.6$" [8]. Romps and Charn come to the result, "This tells us that the standard drag law applies, with a drag coefficient of $c_D = 0.6$. This value of c_D is not far from the value measured for solid spheres moving through a fluid" [9]. In contrast, Morrison et.al. come to a completely different conclusion. They write, "Consistent with the theoretical c_D, the magnitude of drag is small in all simulations. However, whereas the laminar thermals have $c_D \approx 0.01$, the turbulent thermals have weakly negative drag ($c_D \approx -0.1$)" [10]. The negative c_D value is attributed to the accelerating influence of entrainment. The latter article provides a comprehensive overview of various studies on the drag coefficient of thermal updrafts, and hence, no additional quotations are presented here. However, this article is not about the head drag, but about the possible drag of the entire thermal column at right angles to the horizontal wind.

Many of the analyses mentioned above are based on simulations and obviously offer a wide range of interpretations depending on the configuration of the mathematical models. It therefore seems appropriate to take a different approach to the question of whether updrafts lean to the side in the wind, whether they have a drag coefficient and how they move. Here, we deliberately do not use simulation models, but instead evaluate GPS logger data from glider flights, data from boundary layer measuring masts and measurements published in the literature. Based on this real data, a physical description of the behaviour of thermals in the wind is derived.

General considerations from weather observations

First of all, some basic considerations should be made to determine whether thermal updrafts exert any drag on horizontal wind and can be tilted by it. Thermal updrafts are highly stable systems once they attain a certain strength, leaving the superadiabatic layer and forming clouds at altitudes well above a thousand meters. When a glider pilot centers in an updraft, he can almost always follow it up to the cloud base or (in the case

of blue thermals) to the upper end of the convective boundary layer. This holds true even in crosswinds. On some days, the strength and direction of horizontal wind significantly changes with altitude. If thermal updrafts had air resistance against the wind, they would have to drift horizontally at different speeds at various altitudes depending on wind strength. This would inevitably lead to the thermal being torn apart. However, as gliders can circle in thermals even in heterogeneous wind conditions, it seems that such tearing apart does not occur.

Each thermal updraft is surrounded by a downdraft zone all around it, which a glider must pass through before encountering lift [11]. This downdraft area is perceptible from all approach directions and is independent of wind direction and strength. If the thermal tilts in the wind, the surrounding downdraft would have to descend against the horizontal wind direction. It is not very plausible that a thermal updraft yields to the horizontal wind, while its downdraft manages to advance against it. Alternatively, the downdraft zone would have to be significantly displaced, by hundreds of meters, in the lee of the updraft. However, this has not been observed by glider pilots or described in the literature so far.

During the course of the day, depending on the position of the sun and local shielding cloud cover, thermals set in over hundreds of square kilometers at around the same time in the morning. There are days, referred to by glider pilots as "Hammerwetter" (excellent weather), where the sky is covered with cumulus clouds from the Netherlands over northern Germany to Poland, and every 5 to 10 km, a thermal with a diameter of 300 to 500 m is present. Imagine instead of thermals, gigantic cooling towers standing here, reaching up to the clouds. If thermals had a drag coefficient like a cooling tower, it would inevitably influence large-scale wind systems. As thermals initiate, the horizontal wind in the boundary layer would be decelerated, undergoing a left-turning directional change. However, such changes in wind speed and direction are neither perceptible on the ground nor evident in the meteorologists' measurements.

Data evaluation of weather masts

The boundary layer measurement masts in Hamburg-Billwerder (Germany) and Hyytiälä (Finland) make thermals visible. Weather sensors are installed at different heights on the masts. The recorded values for temperature, humidity, wind direction, wind force and ground pressure can be used to generate vertical sections through the lower atmosphere [12].

Figure 2 shows a graphical representation of measurement data from Hamburg Weather Mast on August 20, 2022 in the form of a contour plot [13]. The background color represents wind speed, while white lines indicate isolines of equal potential air density. The representation of potential air density might be somewhat unconventional. In order to eliminate the influence of altitude on air density and thus make it comparable regardless of height, the following conversion was done.

The virtual temperature T_V is the temperature that dry air would have if its pressure and density were equal to those of a given sample of moist air. If this fictitious temperature T_V rather than the actual temperature T_P is used for the moist air of the ascending air parcel, the total pressure p and the density ρ_P of the moist air are related by a form of the ideal gas equation. To apply the equation, the gas constant R_d for dry air is used and the actual temperature T_P is replaced by the virtual temperature T_V [14]:

$$\rho_p = \frac{p}{R_d \cdot T_V} \tag{1}$$

The potential temperature T_{pot} of an air parcel is defined as the temperature that the parcel of air would have if it were expanded or compressed adiabatically from its existing pressure and temperature to a standard pressure p_0 (generally taken as 1000 hPa) [14].

At this point, the calculation should not be made in Kelvin, but in degrees Celsius, so the potential temperature θ in degrees Celsius is $\theta = T_{pot} - T_0 = T_{pot} - 271.35K$. In analogy to the considerations regarding the virtual temperature T_V, it can be assumed that there is a virtual potential temperature θ_V that dry air must have in comparison to moist air with the potential temperature θ at the same density and the same pressure (here p_0). From this, a fictitious "potential air density" ρ_{pot} can be calculated using Eq. 1:

$$\rho_{pot} = \frac{p_0}{R_d \cdot (T_0 + \theta_V)} = \frac{1000\ hPa}{R_d \cdot (T_0 + \theta + \frac{\mu}{6}[^\circ C])} \tag{2}$$

Here the simplified formula proposed by the DWD with one sixth of the mixing ratio μ is used to convert the potential temperature to the virtual potential temperature [15]. The values required for the calculation, including air temperature, humidity, air pressure, and altitude, are derived from the sensor data of the weather mast.

The potential air density is completely pressure-independent as all variables were projected to $p_0 = 1000\ hPa$. This makes the comparison of density differences shown in Fig. 2 much easier: The potential air density is lowest near the ground, because air temperature and humidity in the superadiabatic layer (which is approximately 75 m thick here) are higher than in the layer above. Typical values in Fig. 2 range from 1.171 to 1.175 kg/m³. In the colder layer above, the potential air density is ranging from 1.177 to 1.179 kg/m³. Around 14:07 UTC, a thermal detachment begins, reaching its peak at 14:13 UTC. Light near-surface air ascends upward, extending beyond the top of the measurement mast. Four effects are particularly noteworthy for subsequent considerations:

- Above 100 m, the horizontal wind speed is approximately 8 m/s. During the detachment, within the thermal updraft, it decreases to a minimum of around 4 m/s. Apparently, the updraft is moving at no more than half wind speed.
- The updraft itself is vertical, there is no tilt in the wind.
- Immediately before the detachment of the main thermal, a denser air parcel descends from above at 14:09 UTC, which

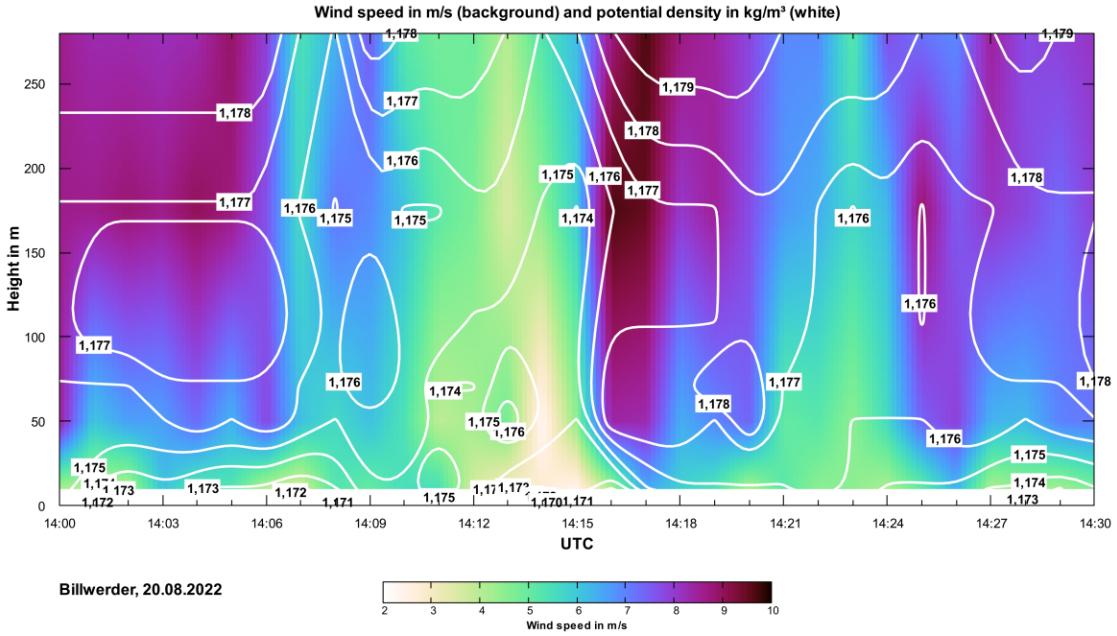

Fig. 2: Graphically processed wind measurement data from the Hamburg Weather Mast during the passage of a large (left) and a small (right) updraft.

then moves beneath the warm, humid, lighter air near the ground at 14:11 UTC and giving it a "kick" upwards.

- Shortly before and especially after the updraft has passed through, the wind speed at higher altitudes increases to up to 10 m/s.

Around 14:23 UTC, another brief detachment occurs, which is notably weaker and triggered by the downdraft bubble around 14:20 UTC.

The phenomena shown here are typical of updrafts that develop in the vicinity of the weather masts at Hamburg-Billwerder and Hyytiälä. They can be observed on any day with thermal convection.

Flight data analysis

Flight data analysis on www.weglide.org

The online portal www.weglide.org offers glider pilots the opportunity to upload their GPS logger files after a flight, visualize it and compare it with the flight paths of other pilots. Several hundred thousand entries from Europe, the USA, Australia and southern Africa have already been collected in this way. This data is also freely accessible to non-pilots [16].

With the permission of WeGlide, flight data was analyzed and screenshots were taken from the portal for this article. Each logger file has a unique number with which it can be identified. The flight numbers used in this article can be found on the Internet at www.weglide.org/flight/<flight number>.

More important than the graphical representation in the WeGlide portal, however, is that WeGlide has released the associated logger files for download. This means that the original aircraft data can be used for a variety of offline analyses. All graphics in this article not being screenshots were obtained by analyzing the raw logger data. This is because a logger file contains line-by-line entries in addition to header data and some other information. Each line of data has a timestamp accurate to the second, so that all other values in the line can be clearly assigned to this time information. These values also include the GPS coordinates with their information on latitude, longitude and altitude.

Updrafts rise vertically

A special feature of WeGlide is the ability to display "wingmen". These are the flight paths of other pilots who were in close proximity for a certain period, for example, circling in the same updraft. In this feature, the paths on the map, as well as the altitude information for each considered flight, are displayed in different colors. This comparison capability is particularly useful for the 3D and time-related analysis of thermal updrafts.

Figure 3 displays the flight paths of two gliders simultaneously circling in the same updraft on a windy day in Northern Germany. The circling of the gliders is clearly visible, including the drift with the wind. The three images depict the altitude and position of the two gliders initially upon entering the updraft (14:46:48 UTC), then at a medium altitude (14:59:29 UTC), and finally at the moment when the red glider reaches its maximum altitude and exits the updraft (14:54:52 UTC). The red pilot is very experienced. His circles are noticeably tighter than those of the blue pilot, and through precise centering, he achieves higher climb rates. The blue pilot is less adept at ascending. Fluctua-

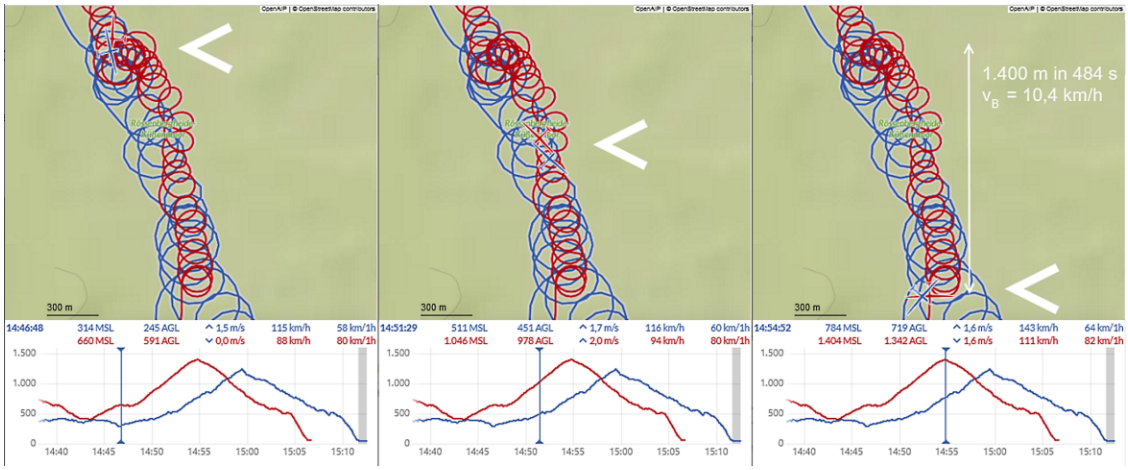

Fig. 3: Two superimposed flight data sets in shared thermal updraft (WeGlide No. 265090, 264946).

tions in the climb rate suggest that he may even "fall out of the updraft" at times and lose altitude. His ascent is significantly slower. Although both start at approximately the same altitude, the blue pilot only reaches 784 m MSL when the red pilot departs at 1,404 m MSL.

Nevertheless, both pilots circle vertically above each other the whole time (i.e. at exactly the same location at the same time), although they are shifted more than 1.4 km to the south by the wind. This behavior is in clear contradiction to Fig. 1, according to which the pilots should have circled offset to each other with an inclined updraft.

This vertical circling is characteristic of thermal updrafts. In WeGlide, no flight paths were found where pilots circle in the same updraft but are offset from each other in a way that would suggest a tilting of the thermal! This holds true for both flatland and mountainous regions.

Figure 4 shows the flight paths of two gliders at two different locations in the Alps. Here, too, the pilots are circling vertically above each other in the same thermal despite considerable wind drift with an altitude difference of several hundred meters.

It is important to point out that, in addition to thermals, there are other types of updrafts that can show a displaced ascent of gliders in WeGlide. In particular, slope winds, atmospheric waves and flying under cloud streets should be mentioned here [1–3]. However, these phenomena are not considered further in this article.

Stationary and moving updrafts

The examples shown above clearly demonstrate the horizontal movement of thermal updrafts with the wind. As already described in the Introduction, this phenomenon has been known for some time. However, WeGlide also provides evidence of stationary updrafts.

Figure 5 illustrates an example. On a day with excellent gliding conditions, allowing flight altitudes up to 2,500 m MSL over the Swabian Alb in Southern Germany, a pilot is ascending at 15:06 UTC (right) in a typical updraft that displaces him with the wind while circling. Ten minutes earlier at 14:49 UTC (left), he is, however, in an updraft that remains completely stationary. Both updrafts are comparably strong and are flown in the same altitude range between 1,700 and 2,200 m MSL. The terrain also does not differ significantly between one updraft and the other. In both cases, the pilot is flying above the relatively flat plateau of the Swabian Alb. In the town of Ennabeuren, there is neither a mountain nor an industrial area that could serve as an excessively intense thermal source and justify a stationary thermal. Apparently, stationary updrafts can occur even in the presence of wind, leading to the hypothesis that the speed at which an updraft travels over the ground is independent of the wind at higher altitudes.

The left updraft shown in Fig. 4 is also nearly stationary. During the approximately 10 minutes in which both gliders circle in it, it only drifts a few hundred meters. It is a typical example of a stationary updraft in the Alps with their steep mountain slopes. The flights on the left and right in Fig. 4 took place on August 20, 2023. Even though the mountains Schiahorn and Galehorn are over 100 km apart, it can be assumed that the upper-level wind at 3,000 to 4,000 m MSL was comparable. The Global Forecast System (GFS) analysis data indicate for both locations at 700 hPa (approximately 3000 m) the same wind speed of approximately 7 km/h from northerly directions. Obviously, there is also a certain wind independence in the drift speed of the thermal.

Further phenomena of moving thermals

The mountain thermal in Fig. 6 (left) is initially stationary. The pilot circles in place, gaining altitude. However, at the marked time, the updraft appears to shift to the south and move towards the Saurüsselkopf. Throughout the entire circling, the pilot is several hundred meters above the terrain and the peaks of neighboring mountains. It therefore cannot be assumed that he was initially circling in a stationary position between two moun-

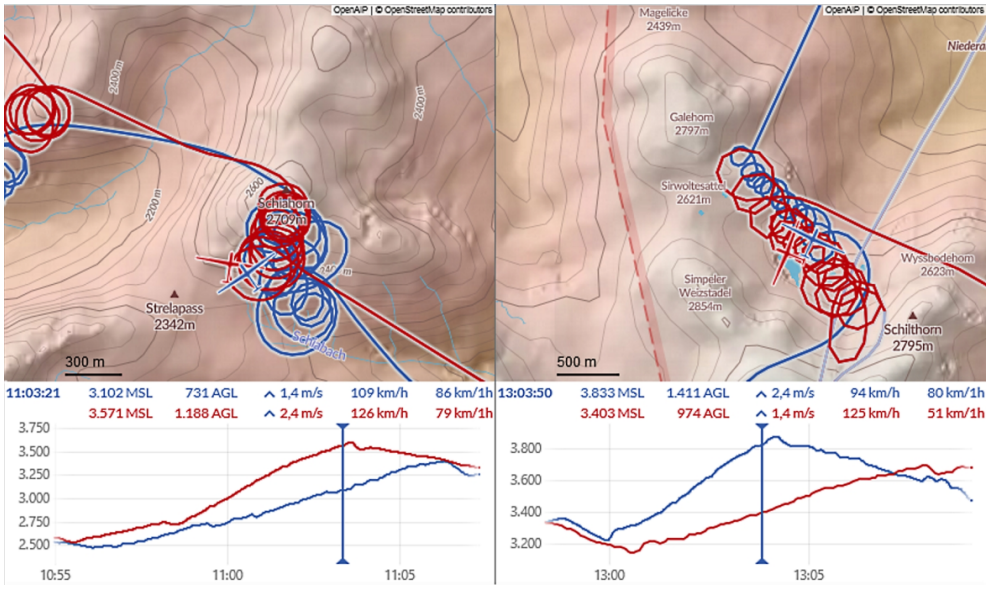

Fig. 4: Two thermal flights in the mountains. On the left a mainly stationary updraft (WeGlide No. 326456, 326243), on the right a moving updraft (WeGlide No. 326259, 326806).

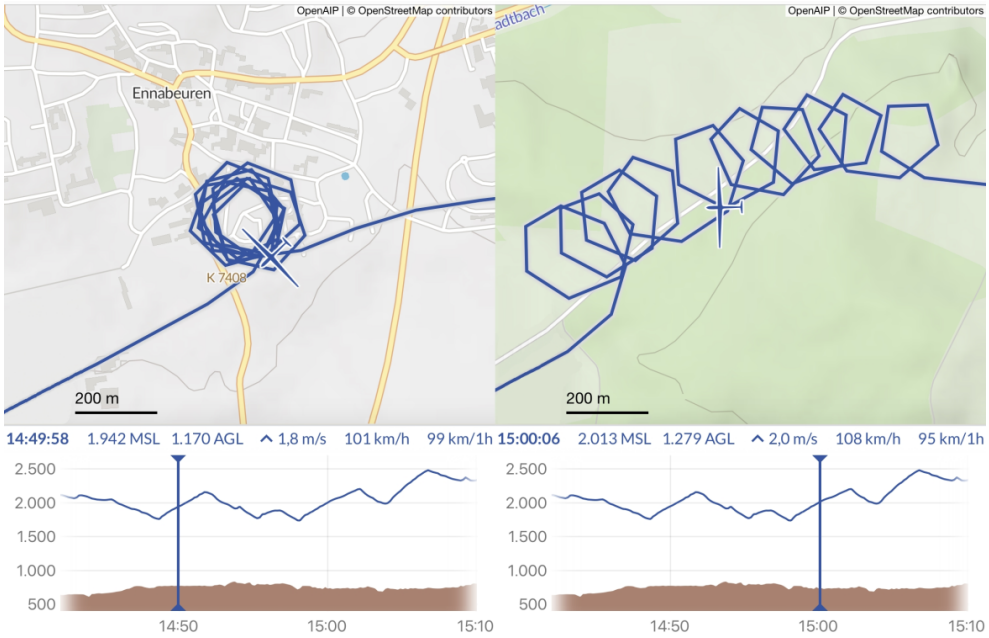

Fig. 5: On the left a stationary updraft, on the right a moving updraft in the same flight within 10 minutes over the Swabian Alb (WeGlide No. 292485).

tains in a valley and was later carried away after having reached the high-altitude wind above the peaks. Thus, the horizontal movement of the thermal is not dependent on the wind at higher altitudes here either.

The flight shown on the right in Fig. 6 demonstrates a clear change in the flight path during circling in the thermal. This change runs parallel to the terrain relief. There was no wave in the lee of the Harz Mountains on this day due to the wind conditions, so that any influence on the updraft in this respect can be excluded. Apparently, the detachment path of the thermal seems to pass through a terrain cut between the hills Bauernberg and Lichtenstein. The pilot circles so high above the terrain that the surrounding wind can no longer be influenced by the terrain profile. The near-ground flow around Bauernberg has a much greater influence on the thermal's track than the higher wind profile.

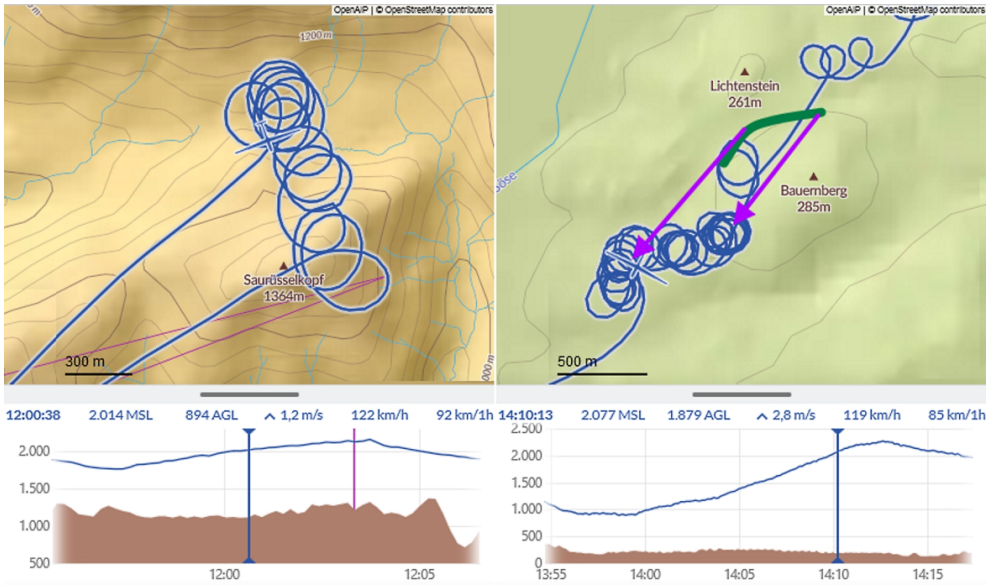

Fig. 6: On the left, an updraft that is initially stationary and then begins to move at the marked time (WeGlide No. 268363). On the right, a moving thermal whose detachment path, marked in green, adapts to the terrain (WeGlide No. 273742).

Both flights in Fig. 6 suggest that the horizontal movement of the thermal is strongly dependent on wind speed and wind direction close to the ground.

Additional sources

An electronic system called "HAWK" is available for gliders, with which the wind forces acting directly on the glider during flight can be calculated and displayed according to wind speed and direction. The measuring principle of HAWK was described in *segelfliegen-magazin*, and the data curve shown in Fig. 7 can be found there [17]. The different colours show the wind values with different filter values. The red curve has the lowest filter, i.e. it shows the wind situation most directly. Towards $t = 80$ s, the pilot flies into an updraft, which can be recognized by the increase in the vertical wind to over 2 m/s. The software algorithm calculates the strength of the horizontal wind at the same time. This drops from an average of 3 m/s to approximately 2 m/s. HAWK thus confirms the phenomenon known from Hamburg-Billwerder (Fig. 2), according to which thermals move horizontally much more slowly than the wind flowing around them.

Paragliders feel the wind more directly than glider pilots because their overall weight is lower, and they hang freely in the lines of their canopy without the enclosure of a cockpit. To prevent the canopy from suddenly collapsing above them, they must remain extremely focused while circling in thermals, especially in stronger updrafts and horizontal winds. For this reason, there are various articles in paragliding literature that delve into the structure of thermals and provide tips for thermal flying. Martens demonstrated that the thermal column has an oval "egg-shaped" cross-section rather than a round one, and it is elongated along the direction of the wind. He notes: "The strong lift is

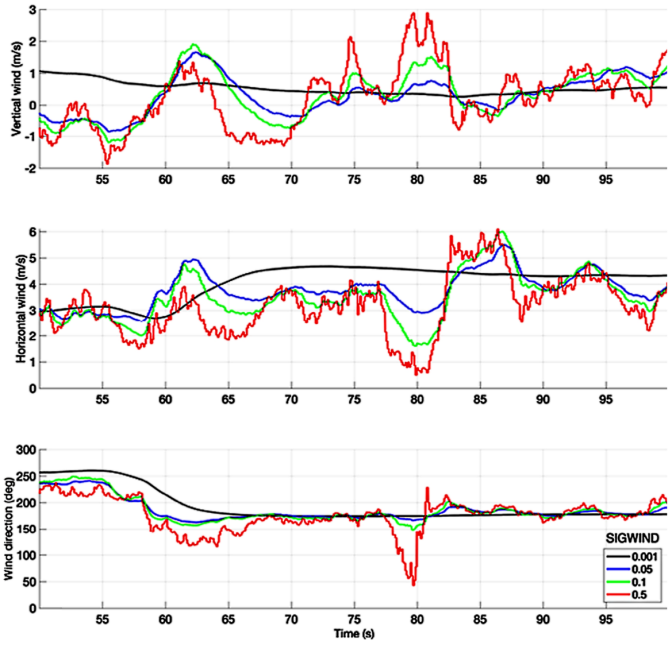

Fig. 7: Measurement of thermal strength (top), horizontal wind (middle) and wind direction (bottom) with HAWK. When entering the thermal at t = 80 s, the wind strength decreases significantly and the wind direction changes. From [17] with kind permission of the author.

very narrow in the windward area and widens toward the leeward area. Therefore, it is better to center tightly. The thermal circles also resemble this egg shape" [18]. Even though the article does not present measurement data, it can be assumed that

the statement, based on flight experience, is accurate.

Various publications show LIDAR data of the convective layer with the aim of measuring updrafts and downdrafts in the atmosphere. Graphical representations of these measurement series can be found, for example, in [19] and [20]. A closer look at these measurements reveals that the thermal updrafts rise vertically upwards. An inclination in the wind is not recognizable. The LIDAR representations are very similar to the Hamburg-Billwerder behavior in Fig. 2, whereby the LIDAR systems cover the entire boundary layer from the ground to the clouds and thus reach significantly higher than the weather mast. This also confirms that the thermals do not tilt in the wind.

Meteorological and aerodynamic interpretation of the observations

The drag coefficient of thermal updrafts in horizontal winds

It is common practice to describe the motion of thermals using Newtonian mechanics. Various examples can be found in the scientific literature where the principles of aerodynamics, specifically those related to air drag, have been applied to thermal phenomena [8, 10, 21]. Additionally, it is not uncommon to employ Newtonian mechanics for the description of other phenomena, such as atmospheric waves [22, 23]. Therefore, classical mechanics also will be used at this point.

Within thermal dynamics, a circular air parcel with a radius r and an incremental height dh is considered (Fig 8). This parcel is enveloped by a wind flowing at a velocity v_W. The air parcel itself possesses two velocity components. It ascends with a presumed constant ascent rate w_P while simultaneously migrating horizontally in the x-direction with a velocity v_B. The air parcel has a volume $V = \pi r^2 \cdot dh$, a density ρ_P, and a mass $m = \rho_P \cdot V$, whereas the ambient air has a density ρ_A. The air parcel experiences the wind force F_W, as well as the inertial force F_I opposing its acceleration (with $\ddot{x}$ being the second derivative of the distance x):

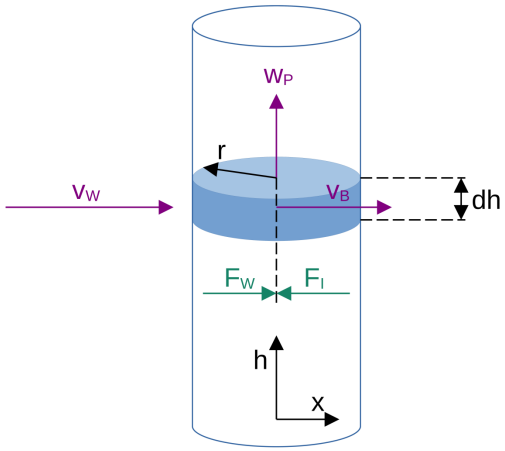

Fig. 8: Velocities and horizontal forces on the model of an ascending air parcel.

$$F_I = m \cdot \ddot{x} = \rho_P \cdot V \cdot \ddot{x} = \rho_P \cdot \pi \cdot r^2 \cdot \ddot{x} \cdot dh \tag{3}$$

$$F_W = \frac{1}{2} \rho_A \cdot c_D \cdot A \cdot (v_W - v_B)^2 = \rho_A \cdot c_D \cdot r \cdot (v_W - v_B)^2 \cdot dh \tag{4}$$

Here c_D represents the sought drag coefficient, and $A = 2r \cdot dh$. As $\ddot{x}$ describes the acceleration of the air parcel in the x-direction and considering force equilibrium $F_W = F_I$, it follows that:

$$\frac{dv_B}{dt} = \frac{\rho_A \cdot c_D}{\rho_P \cdot \pi \cdot r} (v_W - v_B)^2 \tag{5}$$

At this point, it should be explicitly pointed out once again that Eqs. 3 to 5 only describe a phenomenon without, of course, naming the cause. The equations merely show that a body is accelerated in a fluid and that the acceleration depends on the square of the velocity difference. The drag coefficient c_D is simply a mathematical proportionality factor. Whether the acceleration is caused by surface friction, by boundary vortices, by a "pushing" positive pressure difference at the front or a "sucking" negative pressure difference at the rear is not clear from the equation and is completely irrelevant for further consideration. The only central question to be answered by the equations is whether the air parcel is deflected horizontally by the wind flow or not. If this deflection is present, c_D is greater than zero. If there is no measurable deflection, c_D is either negligibly small or zero.

The air parcel detaches from the Earth's surface and ascends because it possesses a lower density compared to the surrounding air. This lower density is attributed, on one hand, to its warmth and, on the other hand, to a higher humidity content in comparison to the surrounding air [24]. Once the upward movement commences, additional moist-warm ground air flows in, giving rise to the formation of a thermal column. Subsequently, this thermal column is envisioned to consist of individual air parcels, each having a height increment dh. Each of these air parcels, assuming a constant uplift velocity w_P, reaches the height h after a certain time t:

$$h = w_P \cdot t \tag{6}$$

Simultaneously, the air parcels are horizontally displaced by the wind. Depending on c_D, the horizontal velocity continuously increases. If $c_D > 0$, this would result in an inclination of the thermal column with increasing height in the direction of the wind (Fig. 9).

In further analysis, the aforementioned "moving thermal" is chosen as a general approach. The detachment point moves at a constant speed $v_{B,0}$, approximately corresponding to the near-surface wind. The particular case of a stationary updraft source arises when $v_{B,0} = 0$ is set.

By integrating Eq. 5, one obtains the respective horizontal velocity of the air parcel at time t, which can be converted into a

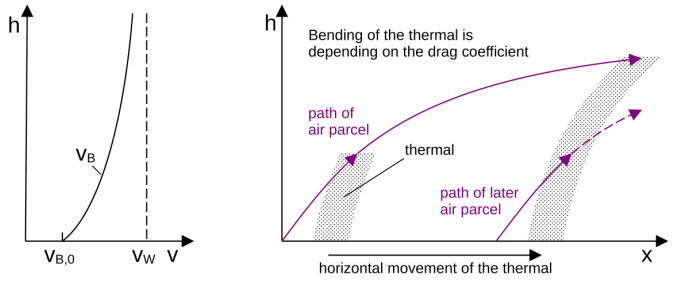

Fig. 9: Rising air parcels in a moving updraft would, if they had a drag coefficient, create an inclined thermal column.

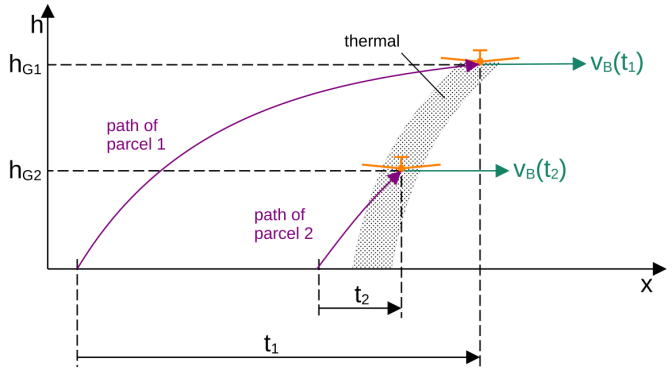

Fig. 10: Position of two gliders in an inclined thermal column according to Fig. 9.

horizontal velocity at height h through Eq. 6. It is

$$v_B(t) = \frac{\rho_A \cdot c_D \cdot v_W (v_W - v_{B,0}) \cdot t + \rho_P \cdot \pi \cdot r \cdot v_{B,0}}{\rho_A \cdot c_D (v_W - v_{B,0}) \cdot t + \rho_P \cdot \pi \cdot r} \quad (7)$$

By performing another integration of Eq. 7, the distance traveled horizontally by the air parcel within a certain time interval can be determined,

$$x_B = v_W \cdot t - \frac{\rho_P \cdot \pi \cdot r}{\rho_A \cdot c_D} \cdot \ln \left[\frac{\rho_A \cdot c_D (v_W - v_{B,0})}{\rho_P \cdot \pi \cdot r} \cdot t + 1 \right] \quad (8)$$

$$x_B = \frac{h}{w_P} v_W - \frac{\rho_P \cdot \pi \cdot r}{\rho_A \cdot c_D} \cdot \ln \left[\frac{\rho_A \cdot c_D (v_W - v_{B,0}) \cdot h}{\rho_P \cdot \pi \cdot r \cdot w_P} + 1 \right] \quad (9)$$

With the help of Fig. 10, we aim to address the question of what drag coefficient c_D a thermal updraft specifically imposes on horizontal wind. As we know from the flight data analyses in the above sections, gliders in an updraft circle vertically to each other. Simultaneously, these circular paths, even if they are separated by hundreds of meters in altitude, are consistently horizontally displaced at the same speed. In Fig. 10, Glider 1 circles at the altitude h_{G1}, and Glider 2 at h_{G2} within the same thermal. As it is a drifting thermal, the air parcels at the location of circling originate from different sources. These air parcels have ascended according to the equations described in Fig. 9. The air parcel at Glider 1 has been in motion for time t_1, while the one at Glider 2 has been in motion for time t_2. Since the horizontal displacement of both gliders occurs at the same speed, $v_B(t_1) = v_B(t_2)$, and thus, according to Eq. 7:

$$\begin{aligned} &\frac{\rho_A \cdot c_D \cdot v_W (v_W - v_{B,0}) \cdot t_1 + \rho_P \cdot \pi \cdot r \cdot v_{B,0}}{\rho_A \cdot c_D (v_W - v_{B,0}) \cdot t_1 + \rho_P \cdot \pi \cdot r} \\ &= \frac{\rho_A \cdot c_D \cdot v_W (v_W - v_{B,0}) \cdot t_2 + \rho_P \cdot \pi \cdot r \cdot v_{B,0}}{\rho_A \cdot c_D (v_W - v_{B,0}) \cdot t_2 + \rho_P \cdot \pi \cdot r} \end{aligned} \quad (10)$$

There are four solutions for Eq. 9:

1. It is $t_1 = t_2$.
   This solution is not appropriate here because $t_1 > t_2$ applies.

2. It is $c_D \cdot v_W (v_W - v_{B,0}) \neq 0$, from which necessarily follows

$$\begin{aligned} \rho_P \cdot \pi \cdot r &= \frac{\rho_A \cdot \rho_P \cdot \pi \cdot r \cdot v_{B,0} \cdot c_D (v_W - v_{B,0})}{\rho_A \cdot C_D \cdot v_W (v_W - v_{B,0})} \\ &= \rho_P \cdot \pi \cdot r \cdot \frac{v_{B,0}}{v_W} \end{aligned}$$

   This would only be possible with $v_W = v_{B,0}$ which does not occur in nature. It is very unlikely that the wind on the ground corresponds exactly to the wind at altitude.

3. It is $c_D \cdot v_W (v_W - v_{B,0}) = 0$ and at the same time $r \cdot v_{B,0} = 0$. With $r \neq 0$ it would only work with $v_{B,0} = 0$ and $v_W = 0$, or with $v_{B,0} = 0$ and $c_D = 0$. A situation with $v_{B,0} = 0$ would be possible in nature, but $v_W = 0$ over the entire height of the convective boundary layer would not, which brings $c_D = 0$ into focus.

4. It is $c_D \cdot v_W (v_W - v_{B,0}) = 0$ and at the same time $c_D \cdot (v_W - v_{B,0}) = 0$, $r \cdot v_{B,0} \neq 0$ and $r \neq 0$.
   This results in either $c_D = 0$ or again the unlikely case $v_W = v_{B,0}$. The latter could also be interpreted in such a way that the rising thermal would no longer be exposed to any further wind force at the time of separation, which would in principle be equivalent to $c_D = 0$.

From these considerations it follows inevitably that $c_D = 0$, or c_D is so small with values of significantly less than 10^{-3} that there is only a negligible displacement of the thermal updraft with height.

The same result is achieved by an alternative approach, as shown in Fig. 11. The first air parcel of a thermal tube reaches point A at $t = t_1$. The thermal has traveled the distance $v_{B,0} \cdot t_1$. There, another air parcel is released, which arrives at point C at time $t = t_2$, while the first air parcel has already climbed to point B. Since it is known from flight analyses that points B and C are strictly vertical to each other, $x_{B1}(2 \cdot t) = v_{B,0} \cdot t_1 + x_{B2}(t_1)$, i.e.

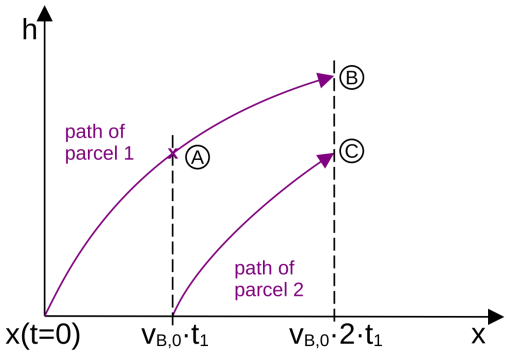

Fig. 11: Temporal relation of two air parcels in a moving vertical thermal updraft.

with the application of Eq. 8,

$$2v_W t_1 \; - \; \frac{\rho_P \pi r}{\rho_A c_D} \cdot \ln\left[2\,\frac{\rho_A c_D (v_W - v_{B,0})}{\rho_P \pi r} \cdot t_1 \; + \; 1\right]$$

$$= \; (v_w + v_{B,0}) t_1 \; - \; \frac{\rho_P \pi r}{\rho_A c_D} \cdot \ln\left[\frac{\rho_A c_D (v_W - v_{B,0})}{\rho_P \pi r} \cdot t_1 \; + \; 1\right] \tag{11}$$

This equation also leads to a $c_D = 0$, or to a negligibly small c_D. Which is, by the way, completely independent of whether the thermal source moves or not ($v_{B,0} = 0$ or $v_{B,0} > 0$).

With $c_D = 0$, Eq. 7 and Eq. 8 simplify to

$$v_B(t) \; = \; v_{B,0} \tag{12}$$

$$x_B(t) \; = \; v_{B,0} \cdot t \tag{13}$$

A parcel of air at altitude h_P has moved forward horzontally during its ascent with a constant velocity $v_{B,0}$ (Fig. 12). For this parcel, its distance from the release point can be easily calculated using Eq. 6. However, the updraft velocity w_P of the air parcel sometimes cannot be measured directly. Instead, the climb rate w_G of a glider within this air parcel is known. Depending on the glider's circling characteristics and the piloting skills, the glider ascends more slowly than the air parcel, with a rough approximation of $w_G \approx w_P - 1$ m/s. Consequently, the horizontal distance travelled by an air parcel ascending in the thermal is thus given by:

$$x_B \; = \; v_{B,0} \cdot \frac{h_P}{w_P} \; \approx \; v_{B,0} \cdot \frac{h_P}{w_G + 1m/s} \tag{14}$$

and for the drift velocity of the thermal column over ground applies,

$$v_B \; = \; v_{B,0} \; = \; \frac{x_B(t_2) \; - \; x_B(t_1)}{t_2 \; - \; t_1} \; = \; const \tag{15}$$

It is important to note that the displacement of the updraft does not depend on the strength v_W of the wind at altitude, but solely on its horizontal speed $v_{B,0}$ near the ground. The magnitude of v_W is completely irrelevant for the traveling speed v_B of the thermal column, as $c_D = 0$.

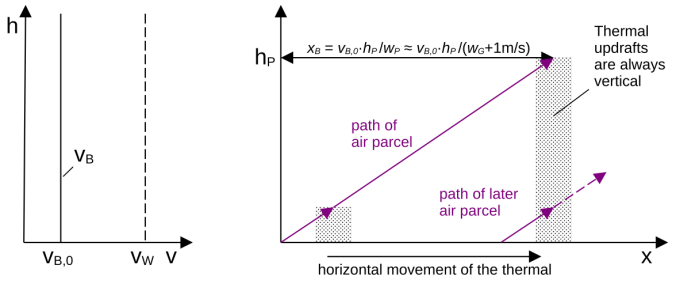

Fig. 12: Distance of an air parcel to its detachment point in a moving vertical thermal.

If the direction of $v_{B,0}$ at the ground changes, the entire thermal column shifts in the new direction. This change can be caused, for example, by a weather-induced shift in the near-surface wind direction or, as shown in Fig. 6, by the terrain's relief influencing the wind.

The influence of horizontal wind on steam and smoke plumes

The dispersion of smoke has been the subject of numerous studies in the literature. Note, all equations from the literature cited here have been transferred to the nomenclature of this article.

Briggs describes the phenomenon where a plume tilts to the side after a certain time in the wind: "The gases are turbulent as they leave the stack, and this turbulence causes mixing with the ambient air; further mechanical turbulence is then generated because of the velocity shear between the stack gases and the air. This mixing, called entrainment, has a critical effect on plume rise since both the upward momentum of the plume and its buoyancy are greatly diluted by this process. The initial vertical velocity of the plume is soon greatly reduced, and in a crosswind the plume acquires horizontal momentum from the entrained air and soon bends over. Once the plume bends over, it moves horizontally at nearly the mean wind speed of the air it has entrained; however, the plume continues to rise relative to the ambient air, and the resulting vertical velocity shear continues to produce turbulence and entrainment." [7]. According to this representation, there is no dedicated force acting on the plume, but rather a momentum transfer takes place. But only in case of entrainment.

Freitas et al. give the following equation for the horizontal wind influence and thus basically follow Briggs' approach [25]:

$$\frac{\delta v_B}{\delta t} \; + \; w_P \frac{\delta v_B}{\delta h} \; = \; -(\lambda_{entr} + \delta_{entr})(v_B - v_W) \tag{16}$$

where λ_{entr} and δ_{entr} are parameters for lateral and dynamic entrainment.

This contrasts with the approach by Robins et al. [26], in which a drag force D acts on the rising plume, with

$$D = \frac{1}{2}\rho_A \cdot c_D \cdot (2\pi r) \cdot (v_B - v_W)^2 \tag{17}$$

and $c_D = 0.21$ is set.

The description of the wind influence using a drag coefficient contradicts Briggs, who writes that: "... the drag term is zero [...]. This is also intuitively evident since one would not expect a vertically rising plume to leave a very extensive wake underneath it" [7].

Regardless of whether momentum transfer or a drag coefficient is at play, it is immediately apparent that both equations are suitable for describing obliquely ascending steam and smoke from chimneys, cooling towers, or large fires, as plumes of steam or smoke do indeed appear to tilt in the wind.

It was mistakenly assumed, and commonly repeated in much of the gliding literature and training curricula, that this tilt also applies to thermals. That "thermals are continuous updrafts like a plume of smoke from a campfire" and "requires the glider pilot to locate the rising thermal current and estimate the amount of slant caused by the winds" [1]. However, thermal updrafts behave fundamentally differently; they rise vertically, unaffected by horizontal wind. Consequently, the equations cited for plume rise cannot be applied to thermal updrafts, or the relevant parameters are null. Obviously, there are other physical effects at work here that require a closer examination.

Interpretation of the causes of the very low drag coefficient

Due to its dimensions, we are in the range of very high Reynolds numbers ($Re > 10^8$), where the drag coefficient of a cylinder is relatively low anyway. Two forces act on a cylinder surrounded by air. One force component arises from the friction of the air stream against the wall surface and is referred to as "friction drag." The second force component results from vortices behind the cylinder, creating a low-pressure area, leading to "pressure drag" (Fig. 13). Both drag components combine to form the overall drag coefficient [27].

It is immediately evident that two conditions must be met for this: on the one hand, the cylinder needs a defined surface (solid or liquid) where air molecules can "hook" and form the separation layer described by Prandtl [28]. On the other hand, the surface of the cylinder must be sufficiently rigid to withstand the low pressure in the wake, preventing the wake from disappearing due to body deformation.

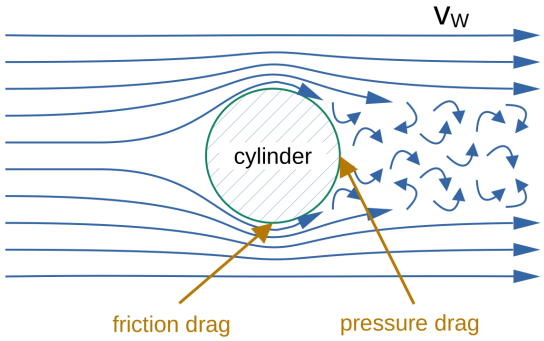

Fig. 13: Schematic representation of flow lines, friction and vortices on a cylinder surrounded by wind.

Smoke (aerosol particles) and steam (water droplets) consist of substances with a defined surface and sufficient stiffness. Even the smallest water droplets have surface tension, making them not arbitrarily deformable. For this reason, the visible components of smoke and steam have indeed a drag coefficient greater than zero. The relationship described in Eq. 17 is thus understandable; smoke and steam must tilt in the wind.

The behavior of thermals is fundamentally different. A thermal column can be considered a relatively "stable" structure. Once formed, it can persist for minutes and only breaks apart at wind speeds above approximately 13 m/s [29]. During the ascent, only a small amount of ambient air mixes with the thermal air. Measurement flights show that lateral entrainment is relatively low [24]. Horizontal wind flows around the thermal without significantly penetrating it. The only effective barrier between the vertically standing "flow channel" of the thermal and the ambient wind is the difference in density. At most, vortex boundaries may form between the thermal and the wind, explaining the lateral entrainment. Thermals have no surface where friction could occur. Simultaneously, the edges of a thermal column are so flexible that no wake is formed, explaining the oval cross-section of the thermal column observed by paraglider pilots. Without friction and wake, the drag coefficient of the thermal column thus is close to zero or zero. The flow around the thermal is shown in Fig. 14. Due to the deflection, the horizontal wind flows around the thermal tube at a higher speed and the streamlines are closer together. However, the ambient wind is not present inside the thermal; only the drift speed of the updraft across the ground is occurring here.

A horizontal line is drawn in Fig. 14. The updraft measured in Fig. 2 could have passed the Hamburg Weather Mast along this line. It should be noted that the updraft moves with the wind. It will have hit the mast first with its right edge, its "rear side", approximately at 14:09 UTC. The time series in Fig. 2 shows the updraft in a horizontal section from "back" to "front". Among other things, one can see the clear increase in wind after the passage of the updraft, as its "head" then passes the mast, where the ambient wind is most strongly deflected and compressed by the thermal column (approximately at 14:16 UTC).

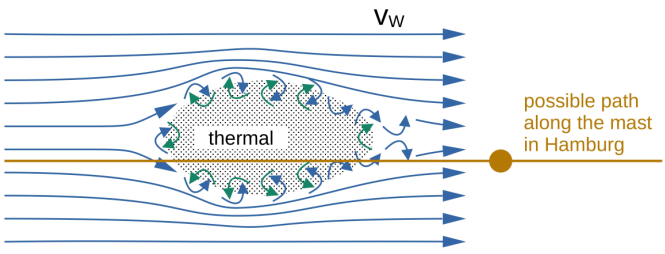

Fig. 14: Schematic representation of flow lines and boundary vortices on a thermal updraft surrounded by wind. The possible drift of the thermal along the Hamburg Weather Mast from Fig. 2 is shown.

The movement, orientation and detachment of thermal updrafts

The calculations in conjunction with countless flight data from gliders prove that thermal tubes have virtually no drag coefficient for the horizontal winds acting on them. This means that Fig. 1 is not correct. Instead, the situation illustrated in Fig. 15 holds true, wherein thermal updrafts ascend vertically and traverse horizontally at the speed they possessed upon detachment from the ground.

You can imagine it like a scarf stretched out long. This scarf represents a near-surface layer of moist and warm air. Upon detachment, one end of the scarf lifts, progressively peeling away from the ground with continuous movement until the scarf ultimately vanishes into a cloud without further ground contact, maintaining the same horizontal velocity throughout the scarf's rise.

Each thermal is moving. As long as the updraft is fueled by near-surface moist and warm air, it will continue to do so. When the supply ceases, the thermal tube detaches from the ground, and its end ascends "free hanging" (Fig. 16). Sailplanes can circle in this rising end. However, if they descend too much, they lose the updraft. It is not uncommon for glider pilots to search unsuccessfully for an updraft several hundred meters below another glider. There, the thermal has already dissipated. In mountainous regions, glider pilots often circle initially in an updraft generated along the ascending mountain slope. When the updraft then dissipates at the mountain ridge, they continue to climb for a short time until the end of the updraft has passed them by.

"Standing" thermals are a special case of moving thermals with $v_B = 0$. If air close to the ground can flow in unhindered, the thermal remains stationary. It then remains vertically above the release point (Fig. 17). This effect is often observed in the mountains, but less frequently in the lowlands.

It should be explicitly emphasized once again that even "stationary" thermals always ascend vertically. They are not inclined in the wind. This arises, on the one hand, from the previously mentioned physical considerations. On the other hand, no flight data could be found in WeGlide where sailplanes circled in the same thermal horizontally and vertically displaced to each other, which they would inevitably be in a tilted thermal column. An experienced glider pilot may note at this point that "industrial thermals," i.e., updrafts generated over cooling towers, appear to be inclined over stationary heat sources. However, a closer examination reveals that these are also moving thermals. The topic, however, is more complex, so a separate section is dedicated to the "cooling tower phenomenon" later on.

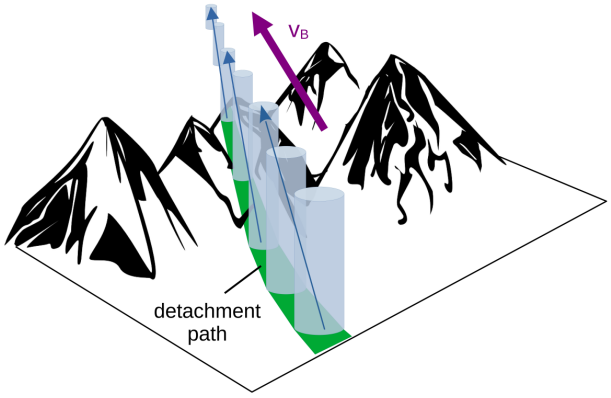

Fig. 16: Detachment path of a moving updraft in the mountains, the thermal breaks off at the mountain ridge, and its lower end rises until the thermal column disappears.

Various navigation software for gliders calculates the wind speed based on the displacement of a glider while circling. However, according to these considerations as illustrated in Figs. 15 and 18, this method is not accurate. These algorithms do not calculate the actual wind speed but rather the drift speed of the thermal over the ground.

Comparison with real flight data

The fact that thermals ascend vertically can be easily verified with logger data from WeGlide. As shown previously, the local offset in wind direction results solely from the drift speed v_B. For many updrafts, $v_B = v_{B,0} = const$ can be used, as the wind conditions near the ground typically do not change during

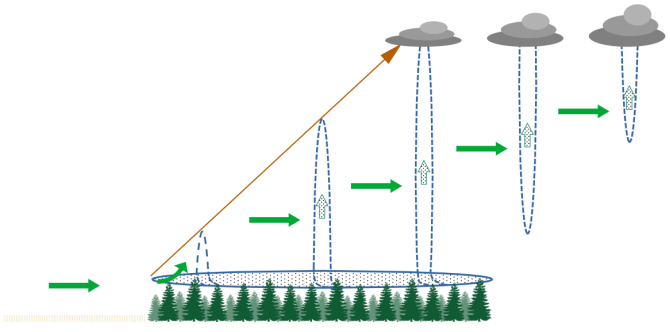

Fig. 15: Lifting and rising of a moist and humid air parcel. A detachment path forms above the treetops.

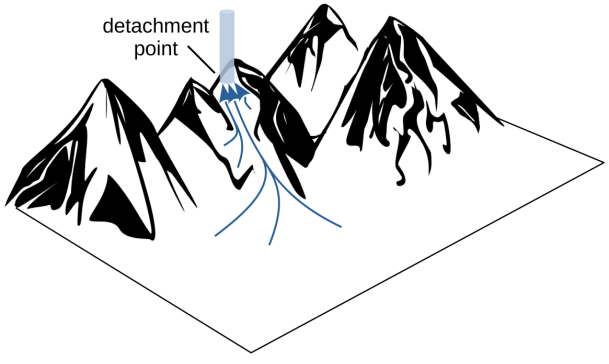

Fig. 17: Formation of a vertically standing updraft through the near-surface inflow of moist-warm air to the "hot spot".

detachment. The uniform displacement can be subtracted using the vertical projection $\Delta x = v_B \cdot \Delta t$ based on Eq. 15. This will make the circling of the glider visible within the moving thermal. From the parameterization of the vertical projection, the drift speed of the updraft can be determined with an accuracy of up to ±0.1 m/s, and the wind direction can be determined to within ±1°. Figure 18 illustrates how the "helix" in which the glider ascends (red) becomes a superposition of concentric circles (blue) by subtracting the thermal column's displacement. It can be observed that the drift speed is apparently constant throughout the entire ascent. If c_D in Eq. 7 had a value greater than zero, v_B would increase with prolonged ascent. This would inevitably lead to the circles diverging and prevent the vertical projection. Since this is not the case, the absence of a drag coefficient is once again confirmed.

One restriction must be considered for the vertical projection: If the wind speed near the ground changes during detachment (as in Fig. 6 left) or if the wind direction near the ground is influenced by terrain structures (as in Fig. 6 right), the vertical projection is not applicable.

The flight path shown in Fig. 18 is part of a glider flight in the Midwest of the USA. Approximately at the same time, a radiosonde ascends in Amarillo. The vertical orientation of the thermal column is not influenced despite significant changes in wind speed and direction at altitude. The updraft remains strictly vertical over an altitude of more than 2000 meters (Fig. 19). The speed of the updraft over the ground and the altitude at which it was flown are shown by the line in blue.

The method of vertical projection can be applied to all updrafts, thus proving that they always ascend vertically. Figures 20 and 21 show two other flights compared to wind data from radiosondes in Bergen (Northern Germany) and Cobar (Australia). Although the radiosondes are at a considerable distance from the flight position, it can be assumed that the wind situation at the aircraft is in principle comparable with the data measured by the sonde. The author, based on personal flight experience, is aware that in the lowlands of Northern Germany, no significant wind differences occur within a 50 km radius of Bergen. Even over the flat, treeless prairies of the USA and over the flat bushland in New South Wales, similar wind forces can be assumed despite the great distances, even if the wind direction may be different.

Applying the method of vertical projection to the flight paths during thermal soaring and utilizing the climb rate of the glider to estimate the thermal strength allows for the determination of the detachment path described in Fig. 16. Figure 22 exemplifies a flight from New Zealand, where sequentially, the two effects of a moving updraft and a stationary updraft are observed. The moving updraft is triggered along a mountainside, with the detachment at the ground following the terrain structure. Shortly before the updraft detaches from the mountain ridge, it drifts from south to southeast according to the shape of the valley where the updraft forms. In contrast, the second updraft is almost stationary. Here, as shown in Fig. 17, thermally capable moist and warm air seems to flow near the ground to a triggering point before ascending vertically. The occurrence of stationary updrafts and moving updrafts on the same day is a phenomenon that is repeatedly observed (see also Fig. 5).

In Fig. 23, more than fifty randomly selected updrafts from WeGlide are evaluated. The gray bars in the right part of the image represent the measured average ground wind and the strength of wind gusts. The blue dots indicate the drift speed of the thermals. The left part illustrates the updraft strength over the drift speed. It can be observed that all three speeds (ground

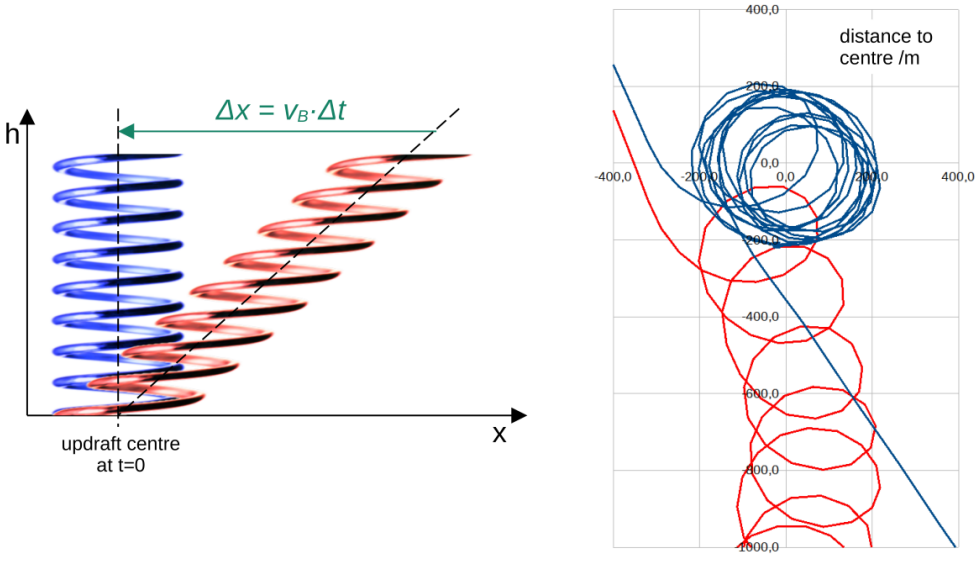

Fig. 18: The vertical projection of the "helix" of a circling glider by subtracting the upwind drift speed v_B shows how the pilot circles in the center of the thermal. Here with WeGlide No. 321555 at 22:48-22:55 UTC, v_B = 5.0 m/s.

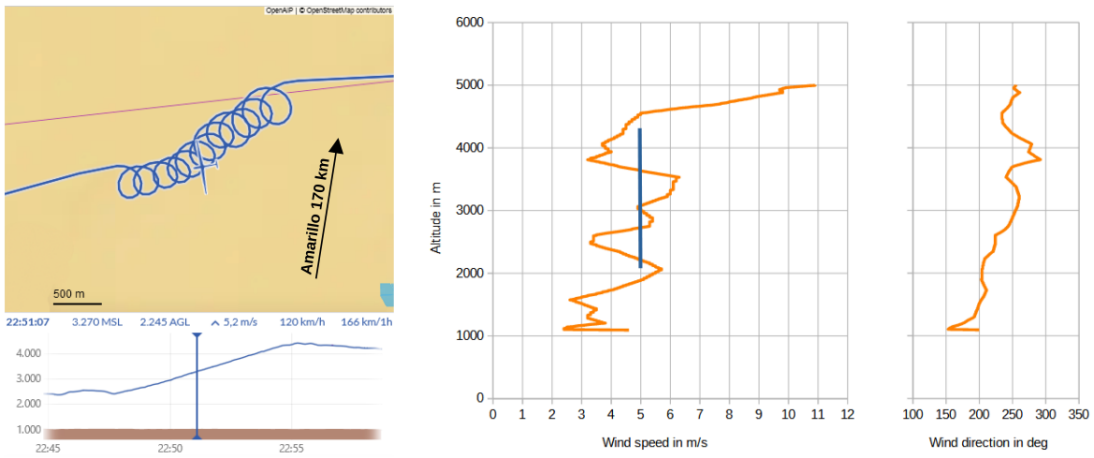

Fig. 19: The updraft from Fig. 18 (in blue) compared to wind data from the Amarillo (USA) radiosonde from 11 Aug 2023 starting 23:01 UTC (in orange) [30].

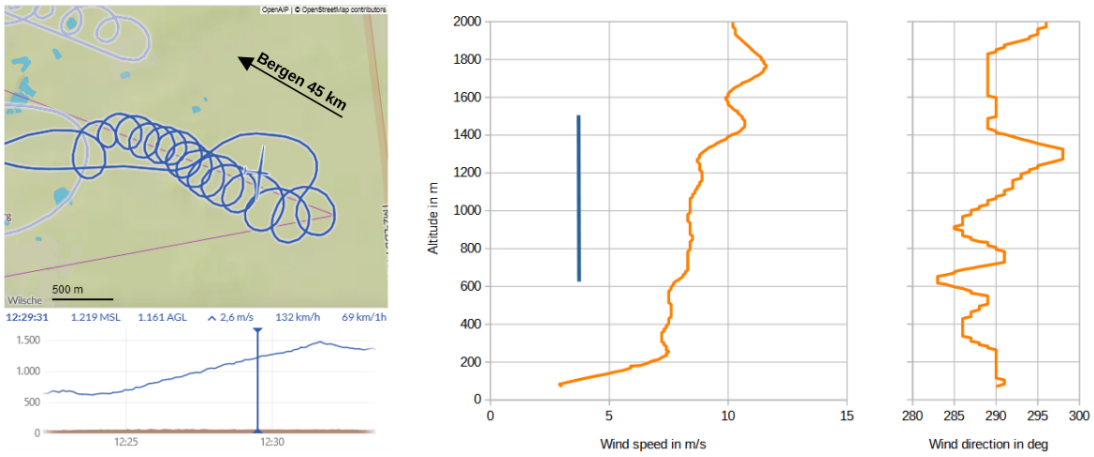

Fig. 20: An updraft from WeGlide No. 185708 with v_B = 4.2 m/s (in blue) compared to wind data from the Bergen (Germany) radiosonde from 15 Jul 2022 starting 12:10 UTC (in orange) [31].

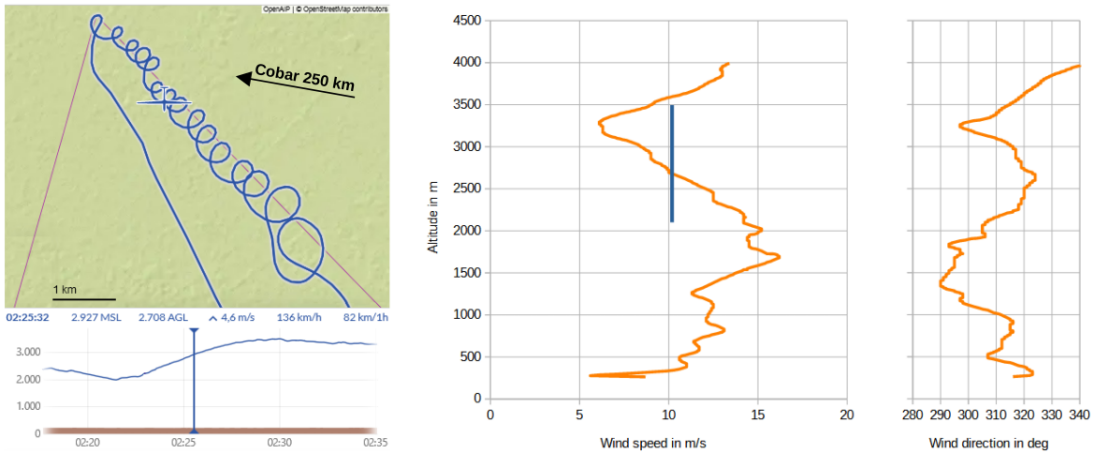

Fig. 21: An updraft from WeGlide No. 351489 with v_B = 10.2 m/s (in blue) compared to wind data from the Cobar (Australia) radiosonde from 08 Dec 2023 starting 23:14 UTC (in orange) [32].

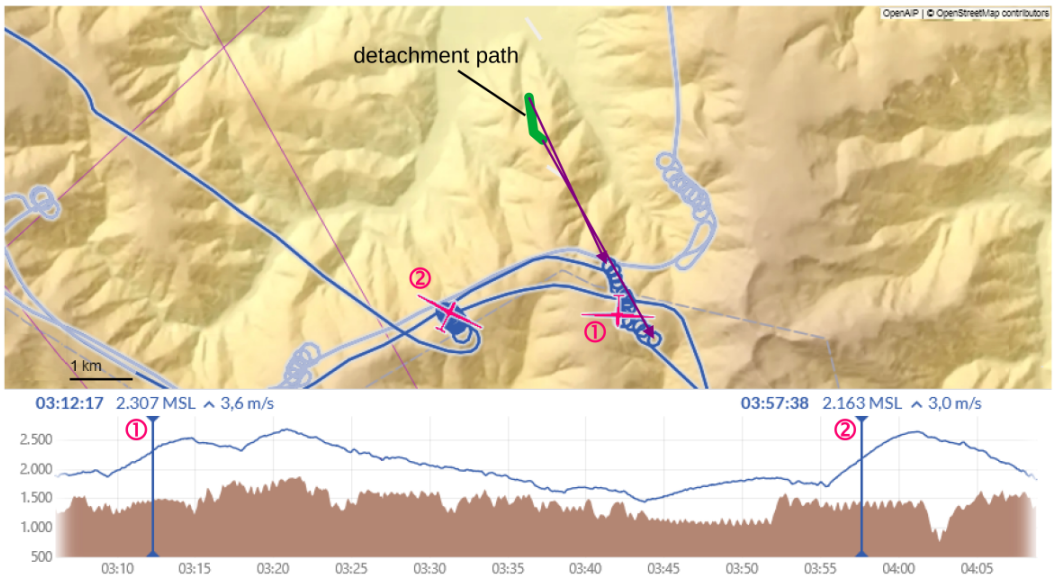

Fig. 22: Two neighboring updrafts, one moving, one standing from WeGlide No. 353093; the detachment path follows the contour of the terrain.

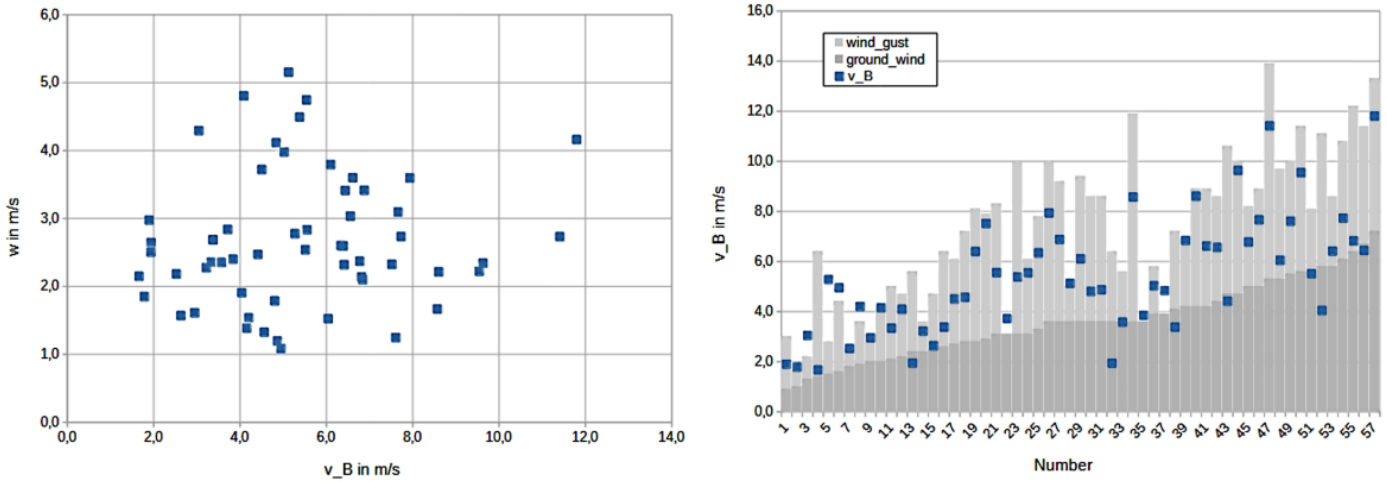

Fig. 23: Comparison of ground wind, wind gusts, thermal strength w, and drift velocity v_B of arbitrary thermals from WeGlide flights; wind data source for thermal locations: [33].

wind, thermal strength, and drift of the updraft over the ground) do not correlate; they are independent of each other. However, there is a relative accumulation of drift speeds between 3 and 7 m/s.

The HAWK system mentioned earlier offers a more detailed understanding of the wind flow around a thermal column. Among other things, the HAWK system records the calculated values for the horizontal wind speed, the wind direction and the strength of the thermal in the logger file. A time stamp makes it possible to clearly assign the wind information to the respective aircraft position. Consequently, these values, along with the associated GPS data, can be found in the WeGlide database if a glider is equipped with HAWK. Figure 24 shows the typical behavior of the air flows, as also were found in other thermal evaluations with HAWK.

Complex offline analyses were carried out for the evaluation shown in Fig. 24. The procedure is described only briefly for reasons of space. The vertical projection (see Fig. 18) is used to transform the helix of the updraft trajectory into concentric circles that rotate around a center point moving with v_B. For this purpose, only those updrafts can be selected from the logger file for which the speed of the surface wind remained constant and its direction was not influenced by the terrain structure. The above-mentioned restrictions for the use of the vertical projec-

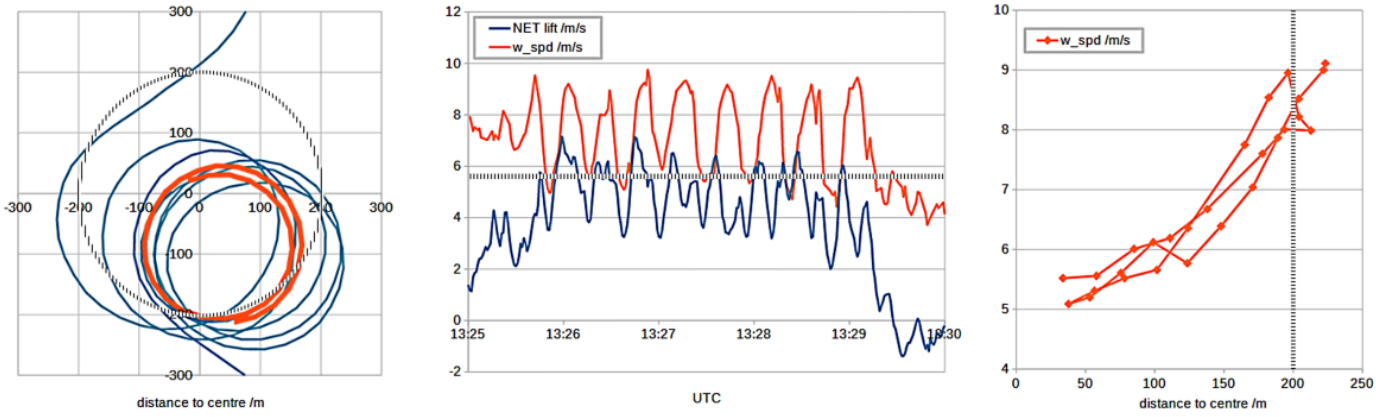

Fig. 24: HAWK data of WeGlide No. 323524; left: vertical projection with v_B = 5.8 m/s; middle: net updraft velocity and horizontal wind speed; right: strength of the horizontal wind at a distance from the updraft center of the circle section marked in orange on the left.

tion must also be considered here. The center of the circle found in this way does not correspond to the center of the thermal updraft, but is offset from it depending on the pilot's skill. Since the pilot sometimes shifts his circling relative to the center of the updraft, the analyses should only be used for a few individual circles and repeated accordingly for other circles. The glider's circular flight path can be interpreted as a cycloid (or roll curve) in relation to the thermal center. The exact position of this center relative to the circular flight path of the glider must be found in several complex parameter variations. The iterative consideration of different criteria helps here. For example, the climb of the glider decreases significantly when it flies beyond the "edge" of the thermal. It is also known from the weather mast data, that the horizontal wind speed decreases towards the center of the thermal and increases towards the edge of the thermal. And finally, all the individual data points in the right-hand section of Fig. 24 must always move uniformly towards the center or towards the edge, without any "loops" in between. Ultimately, the parameter variation results in an optimum for the data shown on the left and right in Fig. 24.

Still referring to Fig. 24, the entry into the updraft occurs at 2500 m MSL with a surrounding wind of approximately 7 m/s. Upon exit at around 3000 m, the surrounding wind is approximately 4.5 m/s. However, while circling in the thermal, a noticeable fluctuation in wind speed is evident. At its minimum, it is slightly over 5 m/s, reaching over 9 m/s at its maximum (Fig. 24, center). The drift speed of the thermal column, determined using the vertical projection, is 5.8 m/s (dashed line in Fig.24, center). Also, the data reveals how the pilot circles within the updraft. The thermal column under consideration has a diameter of approximately 200 m. The pilot is not centrally positioned but rather laterally offset, flying through both the center and the edge of the updraft (Fig.24, left). When plotting the horizontal wind above the thermal radius, it becomes evident how much the surrounding wind increases towards the edge, while inside the updraft only the drift speed of the thermal column is measured (Fig. 24, right). The wind profile shown on the right corresponds to the orange-marked circle in the left part of the image. Thus, the HAWK measurements confirm the flow pattern from Fig. 14, and they depict the same effect observed at the Hamburg Weather Mast with the increasing horizontal wind at the thermal column's edge.

Figure 25 illustrates the detachment of an updraft over a forested area, corresponding to Fig. 15. Where the green line begins, an easterly wind blows into the forest edge behind a clearing. This wind lifts the warm and humid air above the treetops, causing thermal detachment. The resulting updraft ascends vertically and begins to move along the green line in the direction of the wind. It is continuously fueled by the super-adiabatic

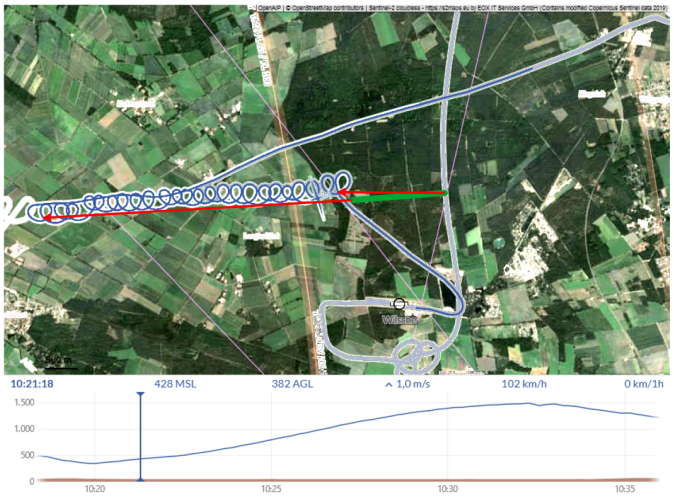

Fig. 25: Detachment path from forest edge to forest edge; the red arrows show where the thermal detached at the beginning and end of the circling (WeGlide No. 256981).

layer, making the thermal column grow taller. At the western edge of the forest, the updraft's supply ceases because the warm and humid air cushion above the trees has ended. The updraft then separates and rises vertically into the clouds, keeping its horizontal speed but losing ground contact. The velocity vectors of the updraft and the thermal's horizontal speed form the sides of a right-angled triangle, enabling the calculation of each rising air parcel's origin along the detachment path.

A glider circles within this thermal. Trigonometric calculations show that the thermal air it enters at 360 m altitude must have detached at the eastern end of the forest (indicated by the right red arrow in Fig. 25). When the glider exits at 1480 m altitude, it is flying in thermal air that detached just before the western edge of the forest (left red arrow in Fig. 25). At this point, the glider's climb rate visibly decreases because the lower detached end of the updraft is passing the glider upwards towards the clouds. The glider can no longer use the updraft. However, the arrows indicate that it has utilized the thermal almost optimally, from the beginning to the end of the detachment path.

Thermals above Cooling Towers

Figure 26 depicts two flights over one of the natural draft cooling towers at the lignite-fired power plant Grevenbroich-Neurath in Germany. Throughout the entire three minutes in which the pilots circle in the "industrial thermal," they fly directly above each other (orange lines). The vertical projection of both flights shows a horizontal drift speed of 4.8 m/s over the ground. The climb rates of the gliders result in an updraft of 4 m/s. The graphical analysis in Fig. 26 suggests that there also may be a "detachment path" here, similar to what is known from natural thermals. This suggestion only appears to contradict the small-scale and locally fixed energy source of a cooling tower.

The cloud of a cooling tower tilts in the wind and soon assumes the same horizontal speed as the ambient wind [7]. One hundred meters behind a cooling tower outlet, the typical droplet diameter is 400 μm with a range of 200 to 600 μm [34]. Chen analyzed the lifespan of various droplet sizes. According to this, droplets with a diameter of 100 μm require approximately 0.2 hours = 720 seconds to evaporate at 80% humidity in a 20 °C warm environment [35]. A 100 μm droplet in Fig. 26 could therefore theoretically fly a distance up to 3,500 m. Larger droplets evaporate more slowly and evaporation is delayed with increasing humidity, whereas it is faster with entrainment turbulence. The detachment path shown in Fig. 26 reaches 1000 m, so it seems plausible.

The relationship between droplet evaporation and thermal development is shown in Fig. 27. The water droplets in the cooling tower cloud evaporate. Entrainment swirls relatively dry ambient air into the cloud, which absorbs the moisture from the evaporating droplets. The turbulence causes this more humid air to return to the environment outside the cloud, where it begins to rise due to its lower density. The rising air draws more ambient air into the cloud, which further increases entrainment and evaporation and creates a thermal column. This reinforcing effect ensures that the thermal can exist for many minutes and ensures that not only individual small bubbles are released from the

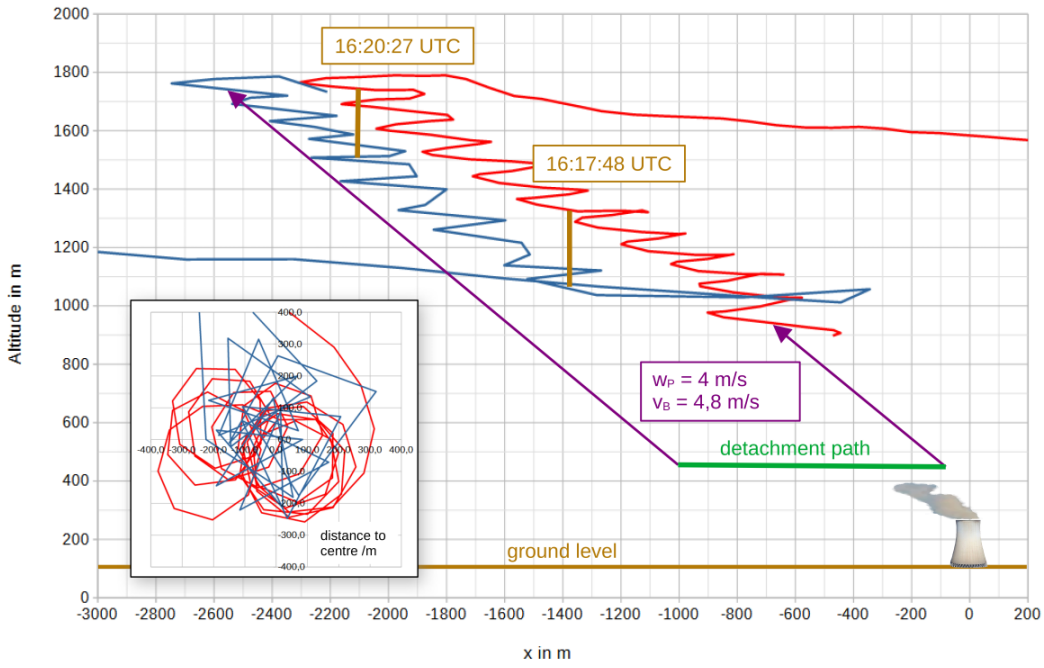

Fig. 26: Between 16:17 UTC and 16:20 UTC, two gliders circle directly above each other in the same updraft from a cooling tower cloud; the updraft rises from a detachment path (WeGlide No. 180635 and 180696). Embedded image: vertical projection with v_B = 4.8 m/s.

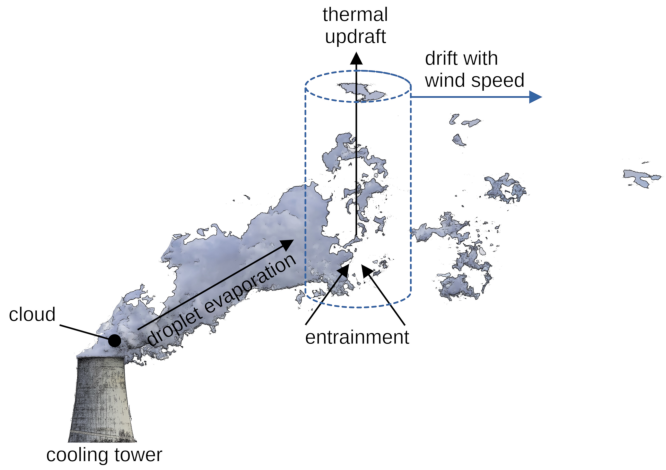

Fig. 27: Formation of a vertical updraft from a cooling tower cloud by vaporization of the water droplets and entrainment.

cooling tower cloud. After all, gliders cannot circle in individual bubbles, and certainly not for minutes at different altitudes directly above each other; they need a dedicated thermal column. Sometimes the detachments become visible through rising cloud fragments above the actual cooling tower cloud. The thermal column moves at the speed of the ambient wind.

The relationships become clear in a Mollier diagram (Fig. 28). On July 4, 2022, the day of the flights shown in Fig. 26, the air pressure at 16:00 UTC at cooling tower outlet height is approximately 1018 hPa, and the ambient temperature is approximately 22.4 °C with a mixing ratio of approximately 6.3 g/kg (point ①), local weather data from [36]). In the studies by Hanna and O'Steen, operating temperatures between 30 and 42 °C are specified for natural draft cooling towers [37, 38]. Therefore, it is assumed for the cooling tower in Neurath that the water used on the working level of the tower evaporates at 35 °C. At 100% relative humidity, this air contains 36 g/kg of water vapour (point ②). During its humid adiabatic ascent with a temperature gradient of approximately 0.6 °C/100 m, some of this water condenses so that the air cools by approximately 1 °C up to the tower outlet and the wet bulb temperature there is approximately 34 °C (point ③). The cooling tower has a height of 173 m [39]. Point ④ shows the state within the cloud above the cooling tower. The air still carries 36 g/kg of water, with point ④ lying at the intersection of the enthalpy line that runs through the associated wet bulb temperature in point ③. The liquid water content (LWC) of the cloud is approximately 2 g/m³, which results from the mixing ratio difference between ② and ③. During the evaporation and mixing by entrainment described in Fig. 27, the state in the cloud moves towards the ambient conditions at point ①. At approximately 25 °C, the droplets almost

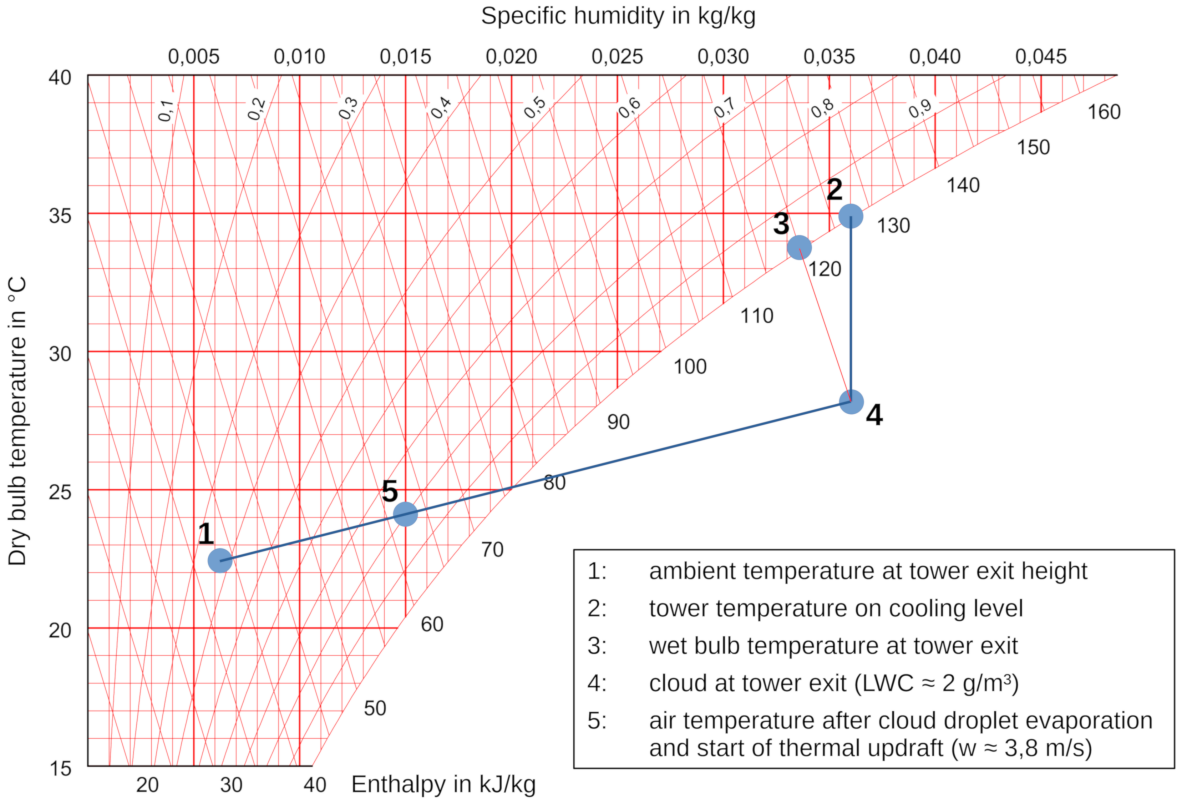

Fig. 28: Mollier diagram with the weather data for Fig. 26 and the resulting thermal strength.

completely evaporate and the relative humidity is around 100%. In this air, should it rise thermally, condensation would immediately occur again due to the cooling caused by the atmospheric temperature gradient. Sometimes these processes can be seen as small cloud-like "eruptions" that swell upwards out of the cooling tower cloud. As the gliders are circling in "clear air", it can be assumed (and the wispy clouds in Fig. 27 indicate this) that the cooling tower air mixes a little more with the surrounding air before it rises as a thermal at point ⑤.

Predelli and Niederhagen were able to demonstrate in their measurement flights that ascending thermal air has no significant temperature advantage over the surrounding air after just a few hundred meters of altitude [24]. Therefore, the crucial factor for the strength of the updraft is the humidity content of the thermal air compared to the surrounding air. If one calculates the corresponding dew point temperatures ($\tau_A = 8°C$, $\tau_P = 19°C$ at $\vartheta_A = 22{,}4°C$) for points ① and ⑤ and applies them to the "thermal formula" presented in [40],

$$w_P \;=\; 5.6\frac{m}{s} \cdot \sqrt{\frac{1.1^{(\tau_P - \tau_A)} - 1}{1.1^{(\vartheta_A - \tau_A)}}} \tag{18}$$

this results in an updraft velocity of $w_P = 3.8$ m/s, which is a good analogy of the value determined in Fig. 26.

Conclusions

Experiences of glider pilots, logger data on weglide.org, measurements from weather masts, LIDAR analyses, and additional sources consistently affirm that thermal updrafts always ascend vertically. They do not tilt into the wind, regardless of how high they may extend within the convective boundary layer. This is confirmed by physical and meteorological considerations. Consequently, thermal updrafts have a drag coefficient of zero or nearly zero concerning the horizontal ambient wind. The vertical thermal column always travels with the horizontal speed that the ascending air parcel had at the moment of detachment from the ground. The detachment path is influenced not only by the near-surface wind but also by the terrain structure, in which the updraft forms. If the horizontal speed at detachment is zero, a stationary thermal column grows vertically above the detachment point.

However, the movement of thermal updrafts requires further analysis. What exactly determines the drift speed? Why can moving and stationary updrafts develop side by side in the lowlands despite a surface wind? What physical relationships explain why, on the one hand, the thermal air remains on the ground until the updraft passes and takes the thermal air up with it and, on the other hand, the thermal air itself starts to move horizontally on the ground in order to merge from different sides and form an updraft? These questions can no longer be answered with logger data from WeGlide; this requires measurement technology close to the ground. The analysis of thermal updrafts still offers great potential for the discovery of new phenomena.

References

[1] Federal Aviation Administration. *Glider Flying Handbook*. U.S. Department of Transportation, 2013. URL: `https://www.faa.gov/sites/faa.gov/files/regulations_policies/handbooks_manuals/aviation/glider_handbook/`.

[2] H. Reichmann. *Streckensegelflug*. Motorbuch Verlag, 10 edition, 2005.

[3] D. Müller and C. Kottmeier. *Meteorologische Aspekte des Streckensegelflugs*. Verlag D. Müller und Ch. Kottmeier, Meteorologische Schriften, 4th edition, 2019.

[4] C. E. Childress. An Empirical Model of Thermal Updrafts Using Data Obtained From a Manned Glider. Master's thesis, University of Tennessee - Knoxville, 2010. URL: `https://trace.tennessee.edu/utk_gradthes/612/`.

[5] B. Eckey. *Streckenflug leicht gemacht*. self-published by the author, 2011. Translation of *Advanced soaring made easy*.

[6] R. Bencatel, J. B. de Sousa, and A. R. Girard. Atmospheric Flow Field Models Applicable for Aircraft Endurance Extension. *Progress in Aerospace Sciences*, 61, 2013.

[7] G. A. Briggs. *Plume Rise*. U.S. Atomic Energy Commission, Division of technical information, 1969. URL: `https://www.osti.gov/biblio/4743102`.

[8] D. Hernandez-Deckers and S. C. Sherwood. A numerical investigation of cumulus thermals. *Journal of the Atmospheric Sciences*, 73(10):4117–4136, 2016. `doi:10.1175/JAS-D-15-0385.1`.

[9] D. M. Romps and A. B. Charn. Sticky Thermals: Evidence for a Dominant Balance between Buoyancy and Drag in Cloud Updrafts. *Journal of the Atmospheric Sciences*, 72(8), 2015. `doi:10.1175/JAS-D-15-0042.1`.

[10] H. Morrison, N. Jeevanjee, and J.-I. Yano. Dynamic Pressure Drag on Rising Buoyant Thermals in a Neutrally Stable Environment. *Journal of the Atmospheric Sciences*, 79(11), 2022. `doi:10.1175/JAS-D-21-0274.1`.

[11] O. Predelli. What goes up must come down. *segelfliegen-magazin*, (3):38–47, 2018.

[12] O. Predelli. Die Entstehung von Thermik am Boden. *segelfliegen-magazin*, (3):14–17, 2023.

[13] I. Lange. Wind and temperature data from Hamburg Weather Mast for July-August 2022. personal communication, May 2023.

[14] J. M. Wallace and P. V. Hobbs. *Atmospheric Science - An Introductory Survey*. Elsevier, 2nd edition, 2006.

[15] DWD. Virtuelle Temperatur und virtueller Temperaturzuschlag. download 2024-01-16. URL: https://www.dwd.de/DE/service/lexikon/Functions/glossar.html.

[16] J. Dibbern. www.weglide.org. download 2024-01-16. URL: https://www.weglide.org.

[17] H. Meyr, P. Huang, and R. Bieri. Wissen woher der Wind weht. *segelfliegen-magazin*, (2):44–51, 2021.

[18] B. Martens. Schnell nach oben – Zentriertechnik. *DHV-info*, pages 40–46, May 2015.

[19] A. Ansmann, J. Fruntke, and R. Engelmann. Updraft and downdraft characterization with Doppler lidar: Cloud–free versus cumuli–topped mixed–layer. *Atmospheric Chemistry and Physics*, 10(16):7845–7858, 2010. doi:10.5194/acp-10-7845-2010.

[20] F. Gibert, J. Cuesta, J.I. Yano, N. Arnault, and P.H. Flamant. On the Correlation between Convective Plume Updrafts and Downdrafts, Lidar Reflectivity and Depolarization Ratio. *Boundary-Layer Meteorology*, 125:553–573, 2007. doi:10.1007/s10546-007-9205-6.

[21] O. Liechti and B. Neininger. ALPTHERM - A PC-based Model for Atmospheric Convection over complex Topography. *Technical Soaring*, 18(3):73–78, 1994. URL: https://journals.sfu.ca/ts/index.php/ts/article/view/621.

[22] D. Etling. *Atmospheric Gravity Waves and Soaring Flight*. Institute of Meteorology and Climatology at Leibnitz University Hannover, 2014. URL: www.schwerewelle.de.

[23] O. Predelli. In der Asse-Elm-Resonanzwelle auf 2.600 m. schwerewelle.de Jahrestreffen, 2020. download 2024-01-16. URL: https://www.schwerewelle.de/jahrestreffen/2020-braunschweig/oliver/Predelli_Asse-Elm-Resonanzwelle.pdf.

[24] O. Predelli and R. Niederhagen. Humidity, the dominating Force of thermal Updrafts. *Technical Soaring*, 45(1), 2021. URL: https://journals.sfu.ca/ts/index.php/ts/article/view/2217.

[25] S. R. Freitas, K. M. Longo, J. Trentmann, and D. Latham. Technical Note: Sensitivity of $1-D$ smoke plume rise models to the inclusion of environmental wind drag. *Atmospheric Chemistry and Physics*, 10:585–594, 2010. doi:10.5194/acp-10-585-2010.

[26] A. G. Robins and D. D. Apsley. Plume Rise Model Specification. Technical Report P11/02Q/17, Cambridge Environmental Research Consultants, 2023. URL: https://www.cerc.co.uk/environmental-software/assets/data/doc_techspec/P11_02.pdf.

[27] T. Baracu and S. Grigoras-Benescu. Computational analysis of the flow around a cylinder and of the drag force. In *The 2nd Conference of the Young Researchers from TUCEB*, 2011.

[28] L. Prandtl. Über die Flüssigkeitsbewegung bei sehr kleiner Reibung. In M. Eckert, editor, *Ludwig Prandtl und die moderne Strömungsforschung*, pages 64–73. Springer, 2023. Originally published in 1904.

[29] M. J. Allan. Updraft model for development of autonomous soaring uninhabited air vehicles. Technical report, NASA Dryden Flight Research Center, 2006. URL: https://ntrs.nasa.gov/citations/20060004052.

[30] download 2024-01-16. URL: http://weather.uwyo.edu/cgi-bin/bufrraob.py?datetime=2023-08-120:00:00&id=72363&type=TEXT:LIST.

[31] download 2024-01-16. URL: http://weather.uwyo.edu/cgi-bin/bufrraob.py?datetime=2022-07-1512:00:00&id=10238&type=TEXT:LIST.

[32] download 2024-01-16. URL: http://weather.uwyo.edu/cgi-bin/bufrraob.py?datetime=2023-12-090:00:00&id=94711&type=TEXT:LIST.

[33] download 2024-01-16. URL: https://www.visualcrossing.com/weather-history.

[34] A. Roffman and L. D. Van Vleck. The state-of-the-art of measuring and predicting cooling tower drift and its deposition. *Journal of the Air Pollution Control Association*, 24(9):855–859, 1974. doi:10.1080/00022470.1974.10469982.

[35] L.-D. Chen. Effects of ambient temperature and humidity on droplet lifetime – a perspective of exhalation sneeze droplets with covid-19 virus transmission. *International Journal of Hygiene and Environmental Health*, 229, 2020. doi:10.1016/j.ijheh.2020.113568.

[36] Meteostat. download 2024-01-16. URL: https://meteostat.net/de/station/D7378?t=2022-07-04/2022-07-04.

[37] S. R. Hanna. Rise and condensation of large cooling tower plumes. *Journal of Applied Meteorology*, 11(5):793–799, 1972. doi:10.1175/1520-0450(1972)011<0793:RACOLC>2.0.CO;2.

[38] L. O'Steen. Plant Vogtle cooling tower studies. Technical Report WSRC-TR-99-00174, US Department of Energy, 2000. doi:10.2172/750910.

[39] R. Wörmann, R. Haupt, and U. Ohlmann. Pilotprojekt der neuen Normengeneration im Kühturmbau – Die Naturzugkühltürme von BoA 2 & 3 in Neurath. *Beton- und Stahlbetonbau*, 103:550–562, 2008. doi:10.1002/best.200800629.

[40] O. Predelli. Thermikprognose mit Temps. *segelfliegen-magazin*, (3):24–28, 2017. URL: https://www.segelfliegen-magazin.de/wp-content/uploads/2021/10/Thermikprognose.pdf.